

# Thin-film flow of a Bingham fluid over topography with a temperature dependent rheology

Miguel Moyers-González<sup>1\*</sup>, James Hewett<sup>2</sup>, Dale Cusack<sup>3</sup>, Ben Kennedy<sup>3</sup> and Mathieu Sellier<sup>2</sup>

<sup>1</sup>School of Mathematics and Statistics, University of Canterbury, NZ. <sup>2</sup>Department of Mechanical Engineering, University of Canterbury, NZ. <sup>3</sup>School of Earth and Environment, University of Canterbury, NZ.

\*mailto: miguel.moyersgonzalez@canterbury.ac.nz

## Abstract

We consider the flow of a viscoplastic fluid on a horizontal or an inclined surface with a flat and an asymmetric topography. A particular application of interest is the spread of a fixed mass – a block – of material under its own weight. The rheology of the fluid is described by the Bingham model which includes the effect of yield stress, i.e. a threshold stress which must be exceeded before flow can occur. Both the plastic viscosity and the yield stress are modelled with temperature-dependent parameters. The flow is described by the lubrication approximation, and the heat transfer by a depth-averaged energy conservation equation. Results show that for large values of the yield stress, only the outer fraction of the fluid spreads outward, the inner fraction remaining unyielded. We also present an analysis which predicts the threshold value of the yield stress for which partial slump occurs.

## 1 Introduction

As the name suggests, a viscoplastic fluid can either behave as a viscous fluid, which deforms continuously when subject to a sufficiently strong mechanical load, or as a solid which undergoes no deformation. As an illustrative example, a volume of viscous fluid deposited on a flat surface will spread under its own weight until the gravity and capillary forces are at equilibrium. A viscoplastic fluid, on the other hand, will only start spreading if the gravity force is strong enough to overcome the fluid cohesive force, which explains why a lump of toothpaste rests on a surface without spreading. The flow/no flow boundary for a viscoplastic fluid is dictated by the yield stress, a rheological property of the fluid. Flow can only occur when the stress within the fluid exceeds the yield stress. Viscoplastic fluids appear in a wide range of contexts including food products (e.g. ketchup, chocolate, peanut butter), healthcare products (e.g. toothpaste, creams), the petroleum industry, cosmetics, geophysical flows, and many others. Lava is a geophysical fluid known to have a viscoplastic behaviour Griffiths (2000), Balmforth *et al.* (2014). A better understanding on the rheology of lava is the motivation behind the work presented here. Specifically, by comparing model results and laboratory/field measurements, we aim to indirectly infer rheological properties of the lava, which would otherwise be difficult if not impossible to measure using standard rheometry techniques. A challenge, however, is that as the lava flows downhill from the eruption site, it cools down by radiation to the surroundings and conduction to the ground and many rheological parameters are temperature-dependent. Building on the work of Bernabeu *et al.* (2016), we develop and implement, a mathematical model describing the flow of a non-isothermal viscoplastic fluid either spreading under its own weight on a horizontal surface or draining down an inclined plane. Of particular interest here is the effect of heat transfer on the spreading and rest state of a viscoplastic slump.



## 2 Mathematical model

A two-dimensional, gravity driven, free surface slump of fluid described by the Bingham rheological law was analysed under isothermal and non-isothermal conditions. Three-dimensional and two-dimensional isothermal thin-film flows of a viscoplastic material have been studied extensively in the past, with a vast range of applications and conditions for its validity, for example see Balmforth & Craster (1999), Balmforth *et al.* (2000), Mei & Yuhi (2001), Balmforth *et al.* (2007), Hogg & Matson (2009), Mitsoulis & Tsamapolous (2017), Hinton & Hogg (2022) and references therein. Recently, Bernabeu *et al.* (2016) considered the temperature-dependent thin-film flow of a Herschel-Bulkley fluid to model lava flow down an arbitrary topography. In order to average and reduce the heat-balance equation, a closure relation is necessary. They assumed that the temperature in the vertical direction can be modelled by a polynomial function of degree three, leading to greater freedom for the temperature profile but also requiring more information to constrain the solution. In this work, we follow instead the original idea of López *et al.* (1996), where they assume a second degree polynomial dependence for the vertical temperature. The result of this assumption appears as a linear reaction term in (2). We found the difference between these approaches to be minimal and controlled via the Péclet number. The resulting unsteady one-dimensional model is

$$h_t + \partial_x \left[ -\frac{h_c^2 [3h - h_c]}{6\mu} (f_x + h_x) \right] = w_s, \quad (1)$$

$$h[\theta_t + \bar{u}\theta_x] - w_s(1 - \theta) - \frac{1}{\text{Pe}}[2a_2 h\theta] = 0, \quad (2)$$

where  $h(x, t)$  is the height of the thin film,  $\theta(x, t)$  the temperature,  $f(x)$  the topography,  $w_s(x)$  the source term, and  $\text{Pe}$  the Péclet number is defined as

$$\text{Pe} = \frac{LU\rho c_p}{k}, \quad (3)$$

where  $L$  and  $U$  are the characteristic length and velocity scales,  $\rho$  the density,  $c_p$  the specific heat capacity, and  $k$  the thermal conductivity. Motion only occurs below the critical height,  $h_c(x, t)$ , with

$$h_c = \max \left( 0, h - \frac{B}{|f_x + h_x|} \right). \quad (4)$$

The rheological parameters are the viscosity,  $\mu(\theta)$ , and Bingham number,  $B(\theta)$ , which are defined by

$$\mu = e^{\alpha_\mu(1-\theta)}, \quad (5)$$

$$B = B_i e^{\alpha_B(1-\theta)}, \quad (6)$$

where  $\alpha_\mu$ ,  $\alpha_B$  and  $B_i$  are constant coefficients. The Bingham number is the ratio between yield stress and viscous stress, and is defined by

$$B = \frac{\tau_y H}{\mu_p U}, \quad (7)$$

where  $\tau_y$  is the yield stress,  $H$  the characteristic height scale, and  $\mu_p$  the plastic viscosity. The averaged velocity,  $\bar{u}(x, t)$ , is given by

$$\bar{u} = -\frac{h_c^2(3h - h_c)}{6\mu h} (f_x + h_x). \quad (8)$$

The coefficient  $a_2(x, t)$  in equation (2) is calculated by solving the following system of equations.

$$\begin{aligned} [(f+h)^2 + 2(f+h) - f^2]a_2(x, t) + [h+1]a_1(x, t) &= 0, \\ \left[ \frac{(f+h)^3 - f^3}{3} - f^2h \right] a_2(x, t) + \left[ \frac{(f+h)^2 - f^2}{2} - fh \right] a_1(x, t) &= h. \end{aligned} \quad (9)$$

We consider homogeneous Dirichlet boundary conditions at the ends of the block for both height,  $h$ , and temperature  $\theta$ . The initial conditions for both the height,  $h_{\text{init}}$ , and temperature,  $\theta_{\text{init}}$ , were prescribed by

$$r(x) = \begin{cases} 1 & -0.5 \leq x \leq 0.5 \\ 0 & \text{otherwise.} \end{cases}$$

### 3 Numerical method

A first order implicit-explicit scheme was employed for time integration, second order derivatives in space were treated implicitly, and expressions (4) to (9) were evaluated explicitly. A second order central difference scheme for equation (1) was used. Equation (2) is hyperbolic, and in order to obtain a stable numerical scheme, the upwind discretisation was applied for the first derivative. The node spacing was  $\Delta x = 10^{-2}$  and the time step was  $\Delta t = 10^{-3}$  for all of the cases. The simulations were run until the block length reached a steady state; determined by evaluating the difference between two successive time steps and comparing with a specified tolerance of  $10^{-7}$ .

## 4 Results

The rheological coefficients for the non-isothermal cases were  $\alpha_B = \alpha_\mu = 0.5$ , whereas the temperature dependence was removed for the isothermal cases by setting  $\alpha_B = \alpha_\mu = 0$ . We let  $w_s(x) = 0$ , and fix  $\text{Pe} = 500$ , which indicates an advection dominated flow.

### 4.1 Horizontal and inclined flat topography

In this section we consider isothermal and nonisothermal flows in flat topographies.

#### 4.1.1 Isothermal steady state and numerical validation

First we present steady state analytical solutions for the isothermal case for the horizontal surface topography. For Bingham fluids, it is known that an arrested state exists, i.e. when all of the material exhibits a balance between the gravitational force, pressure gradient and yield stress. For an extensive discussion about the arrested state see Balmforth *et al.* (2007), Hogg & Matson (2009). The arrested state is fully described by equation (4)

$$h_\infty |f_x + h_x| = B_i, \quad (10)$$

which is true for any domain or topography the material is on. Note that by satisfying the balance in equation (10), the yield surface,  $h_c$ , is equal to zero over the whole domain and there is no flow.

For the case of a flat horizontal and flat topography we have  $f_x = 0$  and the flow is symmetric. Two scenarios exist in this configuration, either the material fully slumps or only partially deforms. In the latter case, part of the material remains unyielded and a *yield-point* exists. We present the two cases below,

1. For a full slump, the solution satisfies

$$\begin{aligned} h_\infty(x_{f,\infty}) &= 0, \\ \int_0^{x_{f,\infty}} h_\infty(x) dx &= \frac{1}{2}. \end{aligned} \quad (11)$$

Therefore

$$h_\infty(x) = \sqrt{2B_i(x_{f,\infty} - x)}, \quad (12)$$

with

$$x_{f,\infty} = \left( \frac{3}{2^{5/2}} \right)^{2/3} B_i^{-1/3}, \quad (13)$$

where  $x_{f,\infty}$  is the position of the front of the slump.

2. For a partial slump we require

$$\begin{aligned} h_\infty(x_{c,\infty}) &= 1, \\ h_\infty(x_{f,\infty}) &= 0, \\ \int_0^{x_{f,\infty}} h_\infty(x) dx &= \frac{1}{2}, \end{aligned} \quad (14)$$

thus,

$$h_\infty(x) = \begin{cases} \sqrt{1 - 2B_i(x - x_c)} & \text{for } x_{c,\infty} < x \leq x_{f,\infty} \\ 1 & \text{for } 0 \leq x \leq x_{c,\infty} \end{cases} \quad (15)$$

with

$$x_{c,\infty} = \frac{1}{2} - \frac{1}{3B_i}, \quad x_{f,\infty} = \frac{1}{2} + \frac{1}{6B_i}. \quad (16)$$

Here,  $x_{c,\infty}$  is steady state the position of the yield point and when it is equal to zero, it provides the required condition to find a critical Bingham number  $B_{i,c}$ , that is the minimum Bingham number for which we have a partial slump, which in this case is  $B_{i,c} = 2/3$ .

In order to validate our numerical method we set  $B_i = 1$ , run the isothermal case to steady state and compare with (15). The results are presented in table 1. The method is first order accurate, and converges to the analytical solution.

$\Delta x$	$\ h - h_\infty\ _\infty$
0.02	0.0153
0.01	0.0079
0.005	0.0041
0.0025	0.0021

**Table 1.** Validation of numerical model, listing the difference between the solution of  $h(t = 300)$  with the analytical steady state  $h_\infty$  from equation (15) under isothermal conditions with  $B_i = 1$ .

#### 4.1.2 Evolution of height and temperature profiles

In this section we compare results of isothermal and nonisothermal spreading dynamics on a horizontal surface, figure 1, and an inclined surface,  $f = m(x_{\max} - x)$  in figure 2. In figures 1(a)-1(d) we present results for the isothermal case for two Bingham numbers,  $B_i = 0.6, 1$ . As we can see arrested state was reached for both Bingham numbers, clearly  $h_c \rightarrow 0$  as  $t \rightarrow \infty$ , see figures 1(b) and 1(d). Note

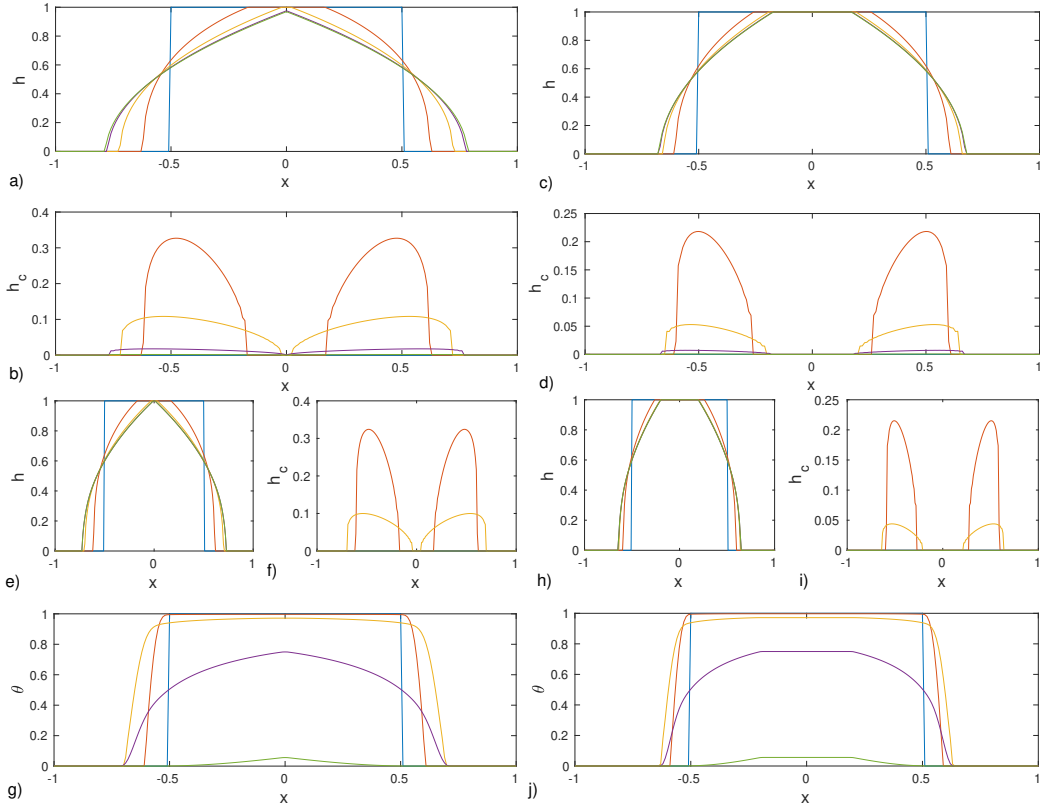


**Figure 1.** Horizontal surface topography ( $f = 0$ ), showing the thin film height  $h(x)$ , critical height  $h_c(x)$ , and temperature  $\theta(x)$  profiles for times  $t = 0, 0.3, 3, 30, 300$ . Isothermal case:  $B_i = 0.6$  for (a) and (b),  $B_i = 1$  for (c) and (d). Non-isothermal case:  $B_i = 0.6$  for (e) to (g),  $B_i = 1$  for (h) to (j).

that for the smaller Bingham number ( $B_i = 0.6$ ) the whole block slumps and spreads until reaching steady state. Conversely, for  $B_i = 1$ , part of the block remains static for all time, i.e. does not deform. As shown in the previous section, there are two flow regimes: (i) no yield point exists and the whole block deforms, figure 1(a), and (ii)  $x_c > 0$  and there is a partial slump, figure 1(c). This is consistent to our previous results since  $B_{i,c} = 2/3$ .

The non-isothermal horizontal profiles of  $h(x)$  and  $h_c(x)$ , shown in figures 1(e), 1(f), 1(h) and 1(i), exhibit similar behaviour to the isothermal case. Note that as  $h_c \rightarrow 0$  the average velocity  $\bar{u} \rightarrow 0$ . Therefore, we expect  $\theta \rightarrow 0$  as  $t \rightarrow \infty$ , which is clearly the case. The Péclet number provides an indication of the ratio between advective and diffusive time scales. The problem analysed in this work is treated as an advected dominated flow, hence a large Pe. The temperature distribution in figures 1(g) and 1(j) has not obtained a steady state even after the film has reached an arrested state. This behaviour is driven by the large but finite Péclet number.

The results for an inclined surface with  $m = 0.2$  are shown in figure 2, where there is no longer a symmetric profile for any of the variables, however, the flow characteristics are similar to the horizontal topography. We confirm previous published results, see Hogg & Matson (2009), and show that an arrested state also exists if  $B_i \neq 0$ . The length of the slump, either full or partial, is larger than in the horizontal problem; true for both the isothermal and non-isothermal cases.

Now we are in a position to investigate the effects that a temperature-dependent rheology has on  $B_{i,c}$ . The maximum height of the block occurs at  $x = 0$ , and the height  $h(0)$  at steady state, effectively  $h_\infty(0)$ , is shown in figure 3(a) for Bingham numbers in the neighbourhood of  $B_i = 2/3$ . The non-isothermal critical Bingham number is less than  $2/3$ . Therefore, the non-isothermal slumps should be shorter in length than the isothermal ones. In order to corroborate this assertion, the length of the steady block as a function of Bingham number for the case of a horizontal surface is shown in figure 3(b). Finally, the influence that the slope  $m$  has on the length of the block was explored for both

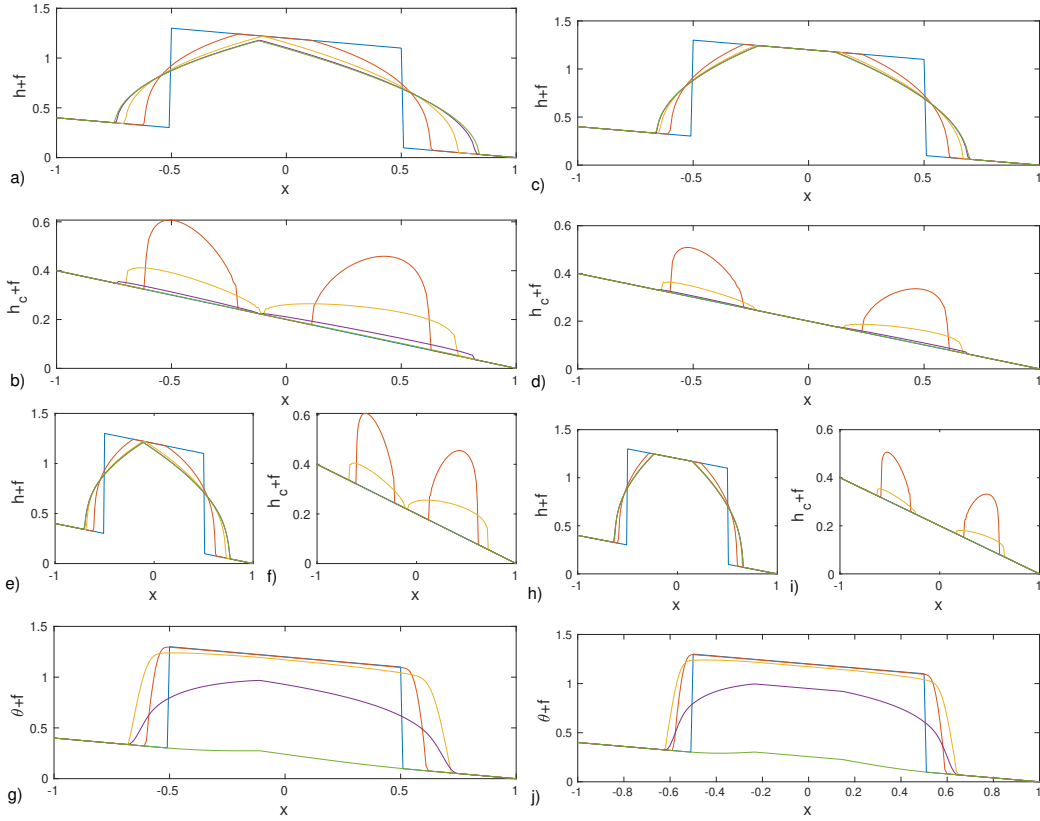


**Figure 2.** Inclined surface topography ( $f = m(x_{\max} - x)$  with  $m = 0.2$ ), showing the thin film height  $h(x)$ , critical height  $h_c(x)$ , and temperature  $\theta(x)$  profiles for times  $t = 0, 0.3, 3, 30, 300$ . Isothermal case:  $B_i = 0.6$  for (a) and (b),  $B_i = 1$  for (c) and (d). Non-isothermal case:  $B_i = 0.6$  for (e) to (g),  $B_i = 1$  for (h) to (j).

isothermal and non-isothermal problems by fixing  $B_i = 1$ , as shown in figure 3(c). Not surprisingly, as  $m$  grows, the length grows in what seems to be a power law manner. Further investigations are underway and remain as future work.

## 4.2 Asymmetric topography

In this section we consider the case of an asymmetric topography, which consists of two equidistant bumps with different heights. Hence,  $f(x)$  is defined in the following way,

$$f(x) = a_l e^{-(x-b_l)^2/c^2} + a_r e^{-(x-b_r)^2/c^2}. \quad (17)$$

We have now centred the block at  $x = 0.5$  and chosen  $a_l = 0.1$ ,  $b_l = -0.1$ ,  $a_r = 0.2$ ,  $b_r = 1.1$ , and  $c = 0.1$ . The values for  $a_l$  and  $a_r$  are carefully chosen such that the lubrication approximation in equation (1) remains valid, see Kalliadasis *et al.* (2000).

In figure 4 we present the results of our simulations. Based on results from previous sections, it is clear that we are asymptotically close to the arrested state if  $t \geq 300$ . Therefore, we plot height,  $h(t, x)$ , and temperature,  $\theta(t, x)$  only for  $t = 300$ . We fix  $B_i = 2/3$  which is the critical Bingham number for the isothermal case. As we can see in figure 4a the symmetry is broken and two distinct yield-points exist. As the block starts to slump,  $f_x(x)$  has opposite sign than  $h_x(t, x)$  at both fronts. This increases yield-stress effects and part of the block never moves, i.e. the critical Bingham number,  $Bi, c$  is less than  $2/3$  now. Clearly, the “new” critical Bingham number will depend on the derivative of  $f(x)$ . As the block spreads, it “climbs” the bumps and stops before reaching the flat ground. Now, even though the sign of  $f_x(x)$  is the same as  $h_x(t, x)$  at the front, is not enough to overcome the effects of

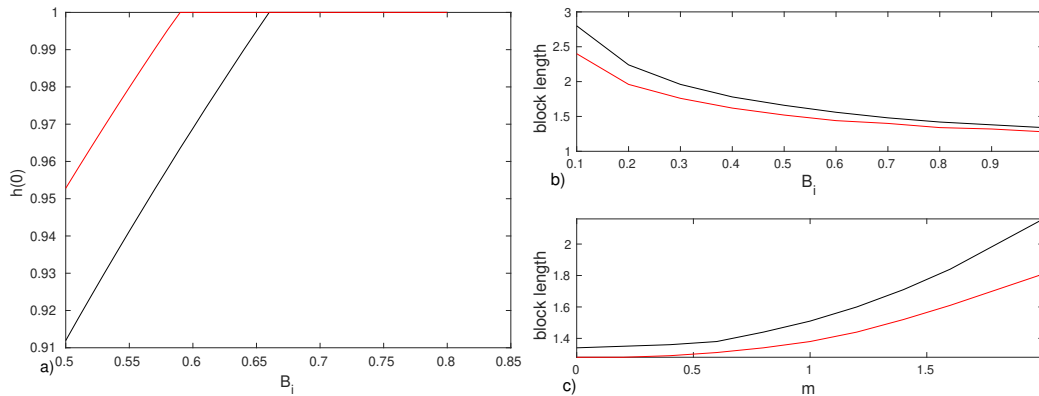


**Figure 3.** (a) Maximum block height ( $h(0)$ ) at steady state for Bingham number close to  $B_{i,c}$ . (b) Steady state block length as a function of Bingham number. (c) Steady state block length for increasing slope and fixed Bingham number  $B_i = 1$ . Isothermal problem (black line) and non-isothermal problem (red line).

the yield-stress. Something similar happens for the nonisothermal case, presented in figures 4b and 4c. The cooling effects increase the unyielded region, where  $h(t, x) \equiv 1$  for all  $t$ , and the spreading of the block slows. As we can see, the block now stops almost at the top of the bumps. Just as in previous sections, thermal effects have an effect in the flow dynamics. This is corroborated in figure 4d where we plot the time series of the length of the block for both cases. As we can see, spreading has reached steady state for both cases and the length of the block for the nonisothermal case is about 6% smaller than the isothermal one.

## 5 Conclusions

The critical Bingham number for the temperature-dependent rheology was smaller than the isothermal counterpart which has  $B_{i,c} = 2/3$ . The length of the viscoplastic block was shorter for higher Bingham numbers and for the non-isothermal case, and longer for steeper inclined slopes. We also investigated the case of an asymmetric topography. As in previous results, thermal effects have the greatest effect on the flow dynamics. The dependence of the arrested state on the non-isothermal behaviour, topographical features, and Bingham numbers has implications for the spreading dynamics of viscoplastic flows.

## Acknowledgements

This work is part of the project ‘‘Indirect measurement of lava rheology’’, Marsden Fund UOC1802. The funding is kindly acknowledged.

## References

- Balmforth, N.J. and Craster, R.V., A consistent thin-layer theory for Bingham fluids, *J. Non-Newtonian Fluid Mech.*, **84**, 1999, 65–81.
- Balmforth, N.J., Burbidge, A.S., Craster, R.V., Salzig, J. and Shen, A., Viscoplastic models of isothermal lava domes, *J. Fluid Mech.*, **403**, 2000, 37–65.
- Balmforth, N.J., Craster, R.V., Perona, P., Rust, A.C. and Sassi, R., Viscoplastic dam breaks and the Bostwick consistometer, *J. Non-Newtonian Fluid Mech.*, **142**, 2007, 63–78.

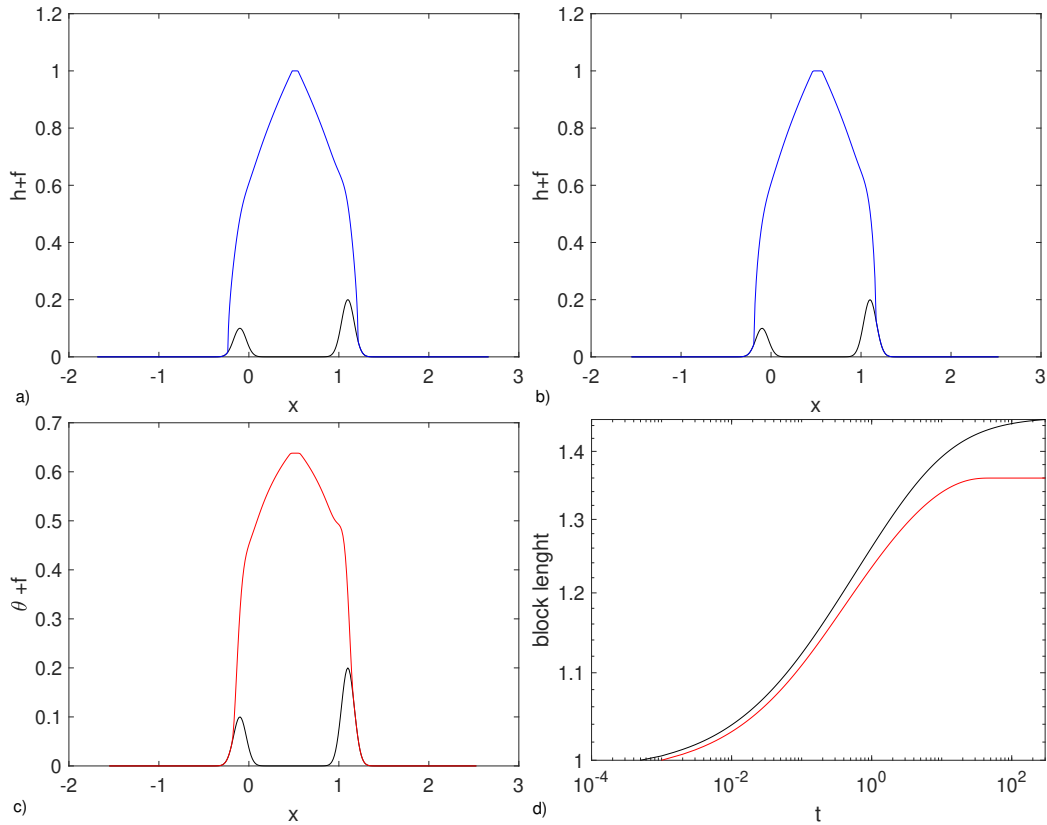


**Figure 4.** Asymmetric topography,  $f(x)$  as in equation 17. (a) and (b)  $h(x)$  for isotherman and nonisothermal case, respectively. (c) temperature  $\theta(x)$  profile. For all cases  $t = 300$  and  $B_i = 2/3$ . (d) Time series for length of the block for both isothermal (black curve) and nonisothermal (red curve) models.

- Balmforth, N J., Frigaard I.A., and Ovarlez G., Yielding to stress: recent developments in viscoplastic fluid mechanics, *Annual Review of Fluid Mechanics* **46**, 2014, 121–146.
- Bernabeu, N., Saramito, P. and Smutek C., Modelling lava flow advance using a shallow-depth approximation for three-dimensional cooling of viscoplastic flows, *Geological Society, London, Special Publications.*, **1**, 2016, 404–423.
- Griffiths, R.W., The dynamics of lava flows, *Annual Review of Fluid Mechanics* **32**, 2000, 477–518.
- Hinton, E.M. and Hogg, A.J., Flow of a yield-stress fluid past a topographical feature, *J. Non-Newtonian Fluid Mech.*, **299**, 2022, 104696.
- Hogg, A.J. and Matson, G.P., Slumps of viscoplastic fluids on slopes, *J. Non-Newtonian Fluid Mech.*, **158**, 2009, 101–112.
- Kalliadasis, S. and Bielarz, C. and Homsy, G.M., Steady free-surface thin film flows over topography, *Physics of Fluids*, **12(8)**, 2000, 1889–1898.
- López, P.G., Bankoff, S. and Miksis, M.J., Non-isothermal spreading of a thin liquid film on an inclined plane, *J. Fluid Mech.*, **324**, 1996, 261–286.
- Mei, C.C. and Yuhi, M., Slow flow of a Bingham fluid in a shallow channel of finite width, *J. Fluid Mech.*, **431**, 2001, 135–159.
- Mitsoulis, E., Tsamopoulos, J. Numerical simulations of complex yield-stress fluid flows. *Rheol Acta* **56**, 2017, 231–258.